Spaceborne potential for examining taiga-tundra ecotone form and vulnerability

P. M. Montesano[1,2], G. Sun[2,3], R. O. Dubayah[3], and K. J. Ranson[2]

[1]Science Systems and Applications, Inc., Lanham, 20706, USA
[2]Biospheric Sciences Laboratory, NASA Goddard Space Flight Center, Greenbelt, 20771, USA
[3]University of Maryland, Department of Geographical Sciences, College Park, 20742, USA

Received: 9 November 2015 – Accepted: 28 November 2015 – Published: 15 January 2016

Correspondence to: P. M. Montesano (paul.m.montesano@nasa.gov)

Published by Copernicus Publications on behalf of the European Geosciences Union.

BGD

doi:10.5194/bg-2015-575

Spaceborne potential for examining taiga-tundra ecotone form

P. M. Montesano et al.

Discussion Paper | Discussion Paper | Discussion Paper | Discussion Paper |

[BGD]

doi:10.5194/bg-2015-575

Spaceborne potential for examining taiga-tundra ecotone form

P. M. Montesano et al.

Abstract

In the taiga-tundra ecotone (TTE), vegetation structure change can be subtle and site-dependent, yet occur across the circumpolar region. This asynchronous change may be related to the horizontal and vertical patterns of vegetation structure such as tree density and height within TTE forest patches (i.e., ecotone form) that is driven by local site conditions and linked to ecotone dynamics. The unique circumstance of subtle, variable and widespread vegetation change warrants the application of spaceborne data including high-resolution (< 5 m) spaceborne imagery (HRSI) across broad scales for examining TTE form and predicting dynamics. Recent work demonstrates the fundamental uncertainty of spaceborne-derived forest structure estimates in sparse boreal forests at the plot-scale. Analyses of forest structure at the patch-scale in the TTE provide a means to examine both vertical and horizontal components of ecotone form, their association with landscape characteristics and environmental factors, and a basis for examining the variation of patch characteristics across sites. In this study we demonstrate the potential of spaceborne data for integrating forest height and density to assess TTE form at the scale of TTE forest patches across the circumpolar biome by (i) mapping forest patches in study sites along the TTE in northern Siberia with a multi-resolution suite of spaceborne data, and (ii) examining the uncertainty of forest patch height from this suite of data across ecotone sites of primarily diffuse TTE forms. Results demonstrate the opportunities for improving patch-scale spaceborne estimates of forest height, the vertical component of TTE form, with HRSI. The distribution of relative maximum height uncertainty based on prediction intervals is centered at ∼ 40 %. We discuss this uncertainty in light of a conceptual model of general ecotone forms. We highlight how the uncertainty of spaceborne estimates of height can contribute to the uncertainty in identifying TTE forms. A focus on reducing the uncertainty of height estimates in forest patches may improve depiction of TTE form, which may help explain variable forest responses in the TTE to climate change and the vulnerability of portions of the TTE to forest structure change.

1 Introduction

1.1 TTE vegetation structure and processes

The transition from continuous forest, to forest patches, to continuous tundra defines the ecological transition zone between boreal forest and tundra, also known as the tree-line, the forest-tundra ecotone, or the taiga-tundra ecotone (TTE). The location, extent, structure and pattern of vegetation in the TTE influences interactions between the biosphere and the atmosphere through changes to the surface energy balance and distribution of carbon (Bonan, 2008; Callaghan et al., 2002a). These TTE vegetation characteristics also affect local and regional arctic and sub-arctic biodiversity (Hofgaard et al., 2012) and are controlled by a variety of factors that are scale-dependent (Holtmeier and Broll, 2005). At local scales the spatial configuration of trees is determined largely by site-level heterogeneity in hydrology, permafrost, disturbance, topography (aspect, slope, elevation), land use and the geomorphologic conditions associated with each (Dalen and Hofgaard, 2005; Danby and Hik, 2007; Frost et al., 2014; Haugo et al., 2011; Holtmeier and Broll, 2010; Lloyd et al., 2003).

In north-central Siberia, where the TTE exhibits a latitudinally defined gradient of tree cover from south to north, TTE forest cover characteristics include a general decrease in height and cover and a variety of spatial patterns (Holtmeier and Broll, 2010). These structural characteristics influence a range of TTE biogeophysical and biogeochemical processes in a number of ways. Recent work notes that rapid growth changes forms, thus altering recruitment dynamics (Dufour-Tremblay et al., 2012). Height and canopy cover of trees and shrubs affect site-level radiative cooling, whereby larger canopies increase nocturnal warming and influence regeneration (D'Odorico et al., 2012). Such tree height and canopy controls over the transmission of solar energy have been well documented (Davis et al., 1997; Hardy et al., 1998; Ni et al., 1997; Zhang, 2004). Vegetation height also influences permafrost, whereby taiga patches trap snow and lower permafrost temperatures (Roy-Léveillée et al., 2014). Recent work also notes the importance of accounting for vegetation heterogeneity in schemes addressing sur-

BGD

doi:10.5194/bg-2015-575

Spaceborne potential for examining taiga-tundra ecotone form

P. M. Montesano et al.

Discussion Paper | Discussion Paper | Discussion Paper | Discussion Paper

face radiation dynamics because of the effects on rates of snowmelt in the boreal (Ni-Meister and Gao, 2011). Modeling results support the importance of tree heights on boreal forest albedo, which is a function of canopy structure, the snow regime, and the angular distribution of irradiance (Ni and Woodcock, 2000). Better representation of vegetation height and cover are needed to improve climate prediction and understand vegetation controls on the snow-albedo feedback in the high northern latitudes (HNL; Bonfils et al., 2012; Loranty et al., 2013). Furthermore, the structure of vegetation in the TTE helps regulate HNL biodiversity, where the arrangement of forest patches provide critical habitat for arctic flora and fauna (Harper et al., 2011; Hofgaard et al., 2012).

1.2   A TTE conceptual model and the scale of observation

Forest ecotones are a form of self-organizing system because there are feedbacks between the spatial patterns of groups of trees and ecological processes (Bekker, 2005; Malanson et al., 2006). The patterns and structural characteristics of TTE forest patches have been conceptualized with a few general and globally recognized ecotone forms (Harsch and Bader, 2011; Holtmeier and Broll, 2010). In the TTE, these general ecotone forms (diffuse, abrupt, island, krummholz) reflect the spatial patterns of forest patches and tree structural characteristics, and have different primary mechanisms controlling tree growth. The variation in ecotone form may help explain regional asynchronicity of TTE forest change because these forms are linked to site factors, the variation in which may in part control the heterogeneity of change seen across the circumpolar TTE (Harsch and Bader, 2011; Lloyd et al., 2002). Further investigation is needed into the link between observed changes in vegetation and local factors that may control these changes (Virtanen et al., 2010).

In the TTE, fine-scale data that resolves individual trees and groups of trees, may help reveal ecotone forms (Danby and Hik, 2007; Hansen-Bristow and Ives, 1985; Hofgaard et al., 2012, 2009; Holtmeier and Broll, 2010; Mathisen et al., 2013). Without resolving groups of individual trees, coarse studies of the land surface may misrepresent ecotone form, be less frequently corroborated with ground data, and disguise the

Discussion Paper | Discussion Paper | Discussion Paper | Discussion Paper |

BGD

doi:10.5194/bg-2015-575

Spaceborne potential for examining taiga-tundra ecotone form

P. M. Montesano et al.

structural heterogeneity of sparse forests. In a TTE landscape this structural hetero-geneity is critical for understanding biodiversity, and biogeochemical and biophysical characteristics such as carbon sources, sinks and fluxes, permafrost dynamics, surface roughness, albedo, and evapotranspiration (Bonan, 2008). Furthermore, understand-ing at a fine-scale where the TTE is likely to change may improve understanding of the potential effects of changing TTE structure on these regional and global processes.

1.3 Spaceborne uncertainty of TTE structure

Spaceborne remote sensing may facilitate linking TTE form with vegetation change and local site factors (Callaghan et al., 2010, 2002b; Harsch and Bader, 2011; Kent et al., 1997). However, a spaceborne assessment of forest structure from single active sen-sors across a gradient of boreal forest structure shows broad ranges of uncertainty at plot-scales (Montesano et al., 2014a, 2015). A spaceborne remote sensing approach that identifies forest patches may provide insight into structural characteristics of forest patches that are indicative of these general ecotone forms at scales that are dictated by the homogeneity of forest structure itself. A patch-based approach to understanding forest height and forest height uncertainty in the ecotone acknowledges the influence that horizontal structure may have on the uncertainty of vertical structure measure-ments from remote sensing. Remote sensing from high resolution spaceborne imagery (HRSI) coupled with spaceborne LiDAR and medium spatial resolution (5–50 m) sen-sors can provide circumpolar observations to evaluate patch characteristics and may provide insight into local-scale ecotone form across the broader circumpolar domain.

1.4 Towards identifying TTE form: spaceborne data integration and scaling

The integration of remote sensing data across patches helps address data scaling issues. First, medium-resolution sensors such as Landsat and ALOS may not be suited for identifying the horizontal patch structure at the resolution required to study TTE structure, however, their spectral or backscatter information may still have value for

Discussion Paper | Discussion Paper | Discussion Paper | Discussion Paper |

[BGD](#)

doi:10.5194/bg-2015-575

Spaceborne potential for examining taiga-tundra ecotone form

P. M. Montesano et al.

predicting patch characteristics. Using the spatial detail of the HRSI to define patch boundaries helps integrate coarser data into an analysis while maintaining the spatial fidelity of patches. Second, patch-level analysis helps attenuate high frequency noise. For example, ALOS PALSAR backscatter has significant pixel-level speckle (Le Toan et al., 2011; Mette et al., 2004; Shamsoddini and Trinder, 2012) which, when grouped with coincident HRSI patch boundaries, can be averaged to reduce this high frequency noise.

A long term goal for monitoring vegetation in the TTE is to not only evaluate the magnitude of change over time and between sites, but also to distinguish portions of the TTE that are vulnerable to changes in structure (i.e. changes in height, canopy cover, tree density) from those whose structure is more resilient, and the rates associated with these changes (Epstein et al., 2004). The spatial patterns of this structural vulnerability will help gap models predict the consequences of TTE structure change on regional and global processes. The short term goal addressed in this study is to examine the uncertainty of mapped forest patch heights using spaceborne remote sensing data integration and to discuss the implication of this uncertainty for both identifying TTE form and predicting dynamics, with regard to separating vulnerable from resilient TTE structure regimes.

2 Methods

2.1 Study area

We visually interpreted HRSI to identify sites in northern Siberia within the TTE where forest cover was sparse and where forest patches exhibited diffuse, abrupt or island ecotone patch forms. The sites are primarily situated on the Kheta-Khatanga Plain, north of the Kheta River, which is a tributary of the Khatanga River flowing north into the Laptev Sea. One site, which sits just south of the Novaya River on the Taymyr

BGD

doi:10.5194/bg-2015-575

Spaceborne potential for examining taiga-tundra ecotone form

P. M. Montesano et al.

Discussion Paper | Discussion Paper | Discussion Paper | Discussion Paper |

Peninsula, includes a portion of Ary-Mas, the world's northernmost forest (Bondarev, 1997; Kharuk et al., 2007; Naurzbaev and Vaganov, 2000).

The region is subject to a severe continental climate, generally exhibits a sparse gradient in tree cover, features elevations generally < 50 m a.s.l., and is underlain with
5   continuous permafrost (Bondarev, 1997; Naurzbaev et al., 2004). The forest cover, exclusively *Larix gmelini*, exists at the climatic limit of forest vegetation, coinciding closely with the July 10 ˚C isotherm (Osawa and Kajimoto, 2009). Sites were chosen based on the presence of cloud-free multispectral and stereo pair data from HRSI available in the Digital Globe archive, and presence of patches of forest cover (Neigh et al., 2013). The
10 geographic footprints of all sites for which forest patches were examined are shown in Fig. 1. Individual tree measurements at circular plots coincident with spaceborne LiDAR footprints were collected during an August 2008 expedition to the south of this study area, along the Kotuykan River, and were used as either calibration or validation data in this study (Montesano et al., 2014b).

15 ## 2.2 Spaceborne data acquisition and processing

A variety of spaceborne remote sensing datasets were used in this study to delineate and attribute forest patches and predict forest patch height. Table 1 lists the individual data sets along with their period of acquisition. These data were collected within ~ 8 year period (2004–2012) across sites during which, based on visual inspection of
20 HRSI, there were no signs of disturbance from fires, and for which the rate of tree growth is likely well below that which would be detectable from spaceborne data in that time interval. The data include passive optical derived from Landsat-7 ETM and Worldview-1 and -2, synthetic aperture radar (SAR) from ALOS PALSAR, and spaceborne light detection and ranging (LiDAR) data from the ICESat satellite's Geoscience
25 Laser Altimeter System (GLAS).

Data consisted of primarily images covering the full extent of each study site that were resampled from their original un-projected format during a re-projection into the Universal Transverse Mercator coordinate system (zone 48). The images were ei-

[BGD]

doi:10.5194/bg-2015-575

Spaceborne potential for examining taiga-tundra ecotone form

P. M. Montesano et al.

ther medium (25–30 m pixels) or high (< 5 m pixels) resolution. The medium resolution spaceborne imagery included the Landsat-7 multispectral composite and vegetation continuous fields tree cover (VCF) products described in Hansen et al. (2013) and ALOS PALSAR tiled yearly mosaics (2007–2010) (Hansen et al., 2013; Shimada et al., 2014). The four ALOS PALSAR yearly mosaics were processed into an average temporal mosaic of dual polarization (HH and HV) backscatter power. The high resolution data consisted of HRSI multispectral (Worldview-2 satellite) and panchromatic (Worldview-1 satellite) data acquired from the National Geospatial Intelligence Agency through an agreement with the US Government (Neigh et al., 2013).

This HRSI was processed in accordance with Montesano et al. (2014) to generate a DSM for each study site (Montesano et al., 2014b). In addition to DSM generation, the HRSI data were processed to compute three other image layers that were used to delineate and attribute forest patches with the mean and variance of corresponding image pixel values. First, a normalized difference vegetation index (NDVI) layer was computed to create a mask separating areas of vegetation from non-vegetation within the HRSI. This widely used algorithm was based on the near-infrared (NIR) and red channels of the multispectral HRSI ((NIR−Red)/(NIR+Red)).

Second, the first of two image roughness datasets was derived for each site. This roughness data was based on the textural characteristics of each site's panchromatic HRSI and was computed using the output layers from the bright and dark edge detection (described in Steps 10–12 of Table 2 in Johansen et al.) (Johansen et al., 2014). The output from this roughness computation was a single image layer showing increased brightness values corresponding to increasingly textured surface features. Within the vegetation mask, a series of thresholds were applied to this layer to create a forest mask sub-category. Forest was separated from non-forest based on a panchromatic HRSI roughness threshold value = 5.5, where higher values represented rougher vegetation and were classified as forest.

Next, the second of two image roughness layers, a canopy roughness model (CRM), was calculated from each DSM. A low pass (averaging) filter (kernal size = 25×25) was

BGD

doi:10.5194/bg-2015-575

Spaceborne potential for examining taiga-tundra ecotone form

P. M. Montesano et al.

applied to a version of the DSM that was resampled to decrease the spatial resolution by a factor of 8. The filtering generated a smoothed terrain elevation (elev$_{terrain}$) layer that removed the elevation spikes from the sparse tree cover that is evident in the DSM. This elev$_{terrain}$ layer was then re-binned to the original spatial resolution. Surface

5 feature roughness was computed as the difference between the DSM and elev$_{terrain}$, and were represented as heights above elev$_{terrain}$. Pixels classified as within the forest mask based on the panchromatic-based roughness input now received a higher level designation and formed the CRM. The panchromatic-based roughness data along with the DSM-based CRM provided two HRSI-derived estimates of vegetation roughness.

10 A CRM threshold value = 1 re-classified existing non-forest regions into the forest class. Finally, remaining non-forest areas with a mean roughness > 3 and mean NDVI < 0.25 was classified as forest, which helped classify remaining vegetation whose roughness value suggested forest vegetation, but whose NDVI value had initially excluded them from this class.

15   The LiDAR data from GLAS featured ground footprint samples of binned elevation returns of features within each footprint. These LiDAR data provided ground surface elevation samples as described in a previous study (Montesano et al., 2014b). The set of GLAS data coincident with the digital surface model (DSM) of the study sites were filtered in an effort to remove LiDAR footprints for which within-footprint elevation

20 changes precluded capturing heights of trees generally less than 12 m tall. GLAS footprints used satisfied the following conditions; (i) the set of coincident DSM pixels had a standard deviation ≤ 5 m, (ii) the length of the LiDAR waveform ≤ 20 m, and (iii) the difference between the maximum and minimum DSM values within a 10 m radius of the GLAS LiDAR centroid was ≤ 25 m.

25 **2.3 Forest patch delineation and attribution**

We analyzed forest structure at the study sites first by delineating forest patch boundaries and attributing these patches with remotely sensed data in order to model forest patch height. This delineation and attribution framework used the segmentation algo-

BGD

doi:10.5194/bg-2015-575

Spaceborne potential for examining taiga-tundra ecotone form

P. M. Montesano et al.

rithms in Definiens Developer 8.7 (Benz et al., 2004). This framework modifies the multi-step, iterative segmentation and classification procedure discussed in previous work (Montesano et al., 2013). The central difference is that this approach uses exclusively data from HRSI to identify a vegetation mask, a subset of which is a forest mask,

5 applies a segmentation to this forest mask to separate distinct forest patches, and then attributes those patches with the mean and standard deviation of pixel values from coincident HRSI, medium resolution Landsat and ALOS PALSAR, and GLAS LiDAR.

The procedure to separate distinct forest patches from within the forest mask involved 2 steps. First, this forest mask was divided to separate portions of forest whose

10 roughness values were > 2 standard deviations above the median roughness value. Next, patches were broken apart according to surface elevation values provided from each site's DSM. Patches were attributed with the mean and standard deviation of image pixel values within the boundary of each patch. Those patches with a minimum size of 0.5 ha were also attributed with coincident LiDAR footprint samples of forest patch

15 height (direct estimates) determined according to an existing approach discussed below.

2.4 Predicting forest patch height directly at LiDAR footprints

Spaceborne LiDAR sampling of forest canopy height provided a means to estimate average patch canopy height through direct spaceborne height measurements. Where

20 forest patches coincide with GLAS footprints, the canopy surface elevation from the DSMs and the ground elevation from either the DSMs or GLAS within a GLAS footprint provide a sampling of forest height within the patch. First, we applied the methodology presented in Montesano et al. (2014) to compile spaceborne-derived canopy height within GLAS footprints and convert those heights to plot-scale maximum canopy height

25 with a linear model (Montesano et al., 2014b). Finally, these plot-scale canopy height predictions from all GLAS footprints within a given patch were used to directly determine the mean predicted forest patch height and the mean height error from the prediction interval of the canopy height linear model.

Discussion Paper | Discussion Paper | Discussion Paper | Discussion Paper |

[BGD]

doi:10.5194/bg-2015-575

Spaceborne potential for examining taiga-tundra ecotone form

P. M. Montesano et al.

2.5 Modeling forest patch height indirectly

Canopy height predictions were made indirectly for forest patches without direct space-borne sampling of forest canopy height. This indirect method, used for the vast majority ($\sim$ 90 %) of forest patches > 0.5 ha across the study sites, involves (i) building a model from the set of forest patches with spaceborne LiDAR samples relating the predicted forest patch canopy height (response variable) to spaceborne image data summarized in Table 1 (predictor variables) and (ii) applying that model to predict forest patch canopy height for those patches with no direct spaceborne height samples. These methods, described in Montesano et al. (2013) and Kellndorfer et al. (2010), use the Random Forest regression tree approach for prediction (Breiman, 2001; Kellndorfer et al., 2010; Montesano et al., 2013). This approach includes specifying the both number of decision trees that are averaged to produce the random forest prediction and the number of randomly selected predictor variables used to determine each split in each regression tree. The result is a prediction model that is valid for the range of predictions on which the model was built and reduces overfitting, or, the degree to which the prediction model is applicable to only the specific set of input data.

3 Results

3.1 Forest patch delineation and direct sample density

The forest patch was the fundamental unit of analysis in this study for which forest height was attributed either directly from spaceborne data at GLAS footprints, or indirectly from spaceborne data by means of empirical modeling with Random Forest. A representative example of patches delineated within the study area in shown in Fig. 2. Across the 9 study sites, 3931 forest patches were delineated based on NDVI, panchromatic texture and DSMs all from the HRSI data. Of this total, 364 patches (9 %) coincided with at least one GLAS footprint at which a height sample was computed and

[BGD](#)

doi:10.5194/bg-2015-575

Spaceborne potential for examining taiga-tundra ecotone form

P. M. Montesano et al.

Discussion Paper | Discussion Paper | Discussion Paper | Discussion Paper

used in the direct estimation of patch canopy height (Fig. 3a). The bimodal distribution that features a peak in the number of forest patches ~ 1 ha in size is evidence of the heterogeneous nature of forest cover in this region. The plots in Fig. 3b group forest patches, for which direct height estimates were made, into categories based on patch area. They show the general distribution of sampling density of direct height estimates within these patches. All patches with direct height samples featured a sampling density of < 3 samples ha^{-1}. The majority (94 %) of sampled patches had sampling densities < 0.5 samples ha^{-1}, of which most had patch areas > 10 ha. Larger patches have lower sampling densities in part because of the irregular arrangement of GLAS tracks across the landscape.

3.2 Forest height calibration and validation comparison

Forest height calibration and validation data were used to build and assess the empirical model for direct spaceborne estimates of height. Figure 4a shows sites for which ground reference calibration and validation data were collected. In Fig. 4b, the corresponding distributions of mean plot/stand height are shown for these sites. Measurements were collected in plots along the Kotuykan River for this study ($n = 69$) and those from regionally coincident stands ($n = 40$) at 6 sites in northern Siberia from Bondarev (1997).

A portion of the Kotuykan River plots were used to calibrate ($n = 33$) the model used to estimate spaceborne canopy height at plot-scales after Montesano et al. (2014), which was applied in the direct spaceborne estimation of forest patch height (Montesano et al., 2014b). The remaining portion of the Kotuykan River plots ($n = 36$) and stands from Bondarev (1997) ($n = 40$) serve as independent validation of the distribution of forest patch heights derived from direct spaceborne height estimation (Bondarev, 1997). Mean heights of forest patches, plots, and stands are used to compare distributions of calibration and validation data because this was the height metric that was consistently available across the set of forest patches, the calibration plots and the validation plots and stands. The distributions in Fig. 4c show the proportion of forest

Discussion Paper | Discussion Paper | Discussion Paper | Discussion Paper |

BGD

doi:10.5194/bg-2015-575

Spaceborne potential for examining taiga-tundra ecotone form

P. M. Montesano et al.

patch heights of those for which direct spaceborne estimates of height were made. This distribution of direct spaceborne estimates of forest patch heights is shown alongside the distributions of individual tree measurements averaged across plots or stands from (i) the calibration plots in Montesano et al. (2014), (ii) the remaining Kotuykan River validation plots, and (iii) the validation stands from Bondarev (1997).

3.3 Indirect forest patch height estimates

Indirect spaceborne estimates of forest patch heights were made for the majority of patches examined. Maximum and mean forest heights were predicted for 91 % of forest patches across the study sites. Random Forest regression tree models for 5 sets of spaceborne data predictor variables were used to estimate maximum and mean patch height indirectly for patches with no coincident direct spaceborne height estimates. Figure 5 shows the residual standard error (RSE) and R^2 of the best performing model (based on R^2) for each spaceborne data predictor set (a particular combination of spaceborne data). The predictor set "All" that included all spaceborne data layers (HRSI multispectral, HRSI panchromatic, HRSI DSMs and CSR, Landsat products, ALOS PALSAR mosaic) explained > 60 % of overall variation in modeled patch height. This "All" model shows only incremental improvement over the model using only HRSI-derived predictors. The Landsat and ALOS spaceborne variables explain < 40 % of variation within the modeled relationship between spaceborne predictors and patch height.

3.4 Uncertainty of forest patch height estimates

We assessed the best performing Random Forest model for indirectly estimating maximum and mean forest patch heights. The best performing models were those from the "All" predictor sets, described above, where the number of predictor variables was 14 and 15, for maximum and mean forest patch height, respectively. Assessments were based on model R^2 and RMSE for the maximum and mean patch height mod-

Discussion Paper | Discussion Paper | Discussion Paper | Discussion Paper |

BGD

doi:10.5194/bg-2015-575

Spaceborne potential for examining taiga-tundra ecotone form

P. M. Montesano et al.

els, where 50 % of patches with direct height estimates from which the indirect models were built were used for model training and 50 % were used for model testing. The results of a bootstrapping procedure to examine the distribution of R^2 and RMSE from the Random Forest models applied to the set of testing data is shown in Fig. 6a, b. The

5 plots show the bootstrapped distributions of best performing model R^2 and RMSE, and are overlain with boxplots. The Random Forest models for maximum and mean patch height explain 61 % (±14 % at 2 σ) and 59 % (±14 % at 2 σ) of the variation with errors of 1.6 m (±0.2 m at 2 σ) and 1.3 (±0.2 m at 2 σ), respectively, where 2σ represents the 95 % confidence interval.

10 We computed 95 % prediction intervals for patches receiving both direct and indirect height estimates. These prediction intervals show the uncertainty associated with patch-level estimates of both maximum and mean patch heights. Figure 7a shows these height estimates and prediction intervals for all patches in this study across the continuum of patch sizes. Figure 7b shows the relative prediction error, which was com-

15 puted as the difference between the upper and lower prediction interval range divided by the predicted height value.

4 Discussion

Site-scale monitoring of forest structure will help quantify the potential for change in forest structure and the effects on broader TTE dynamics. Such detailed monitoring

20 is needed to resolve both the variability in TTE forest structure at fine spatial scales and the variability in structural responses to changes in environmental drivers that are observed across the TTE. The high resolution delineation of forest patches at our study sites in the TTE of northern Siberia demonstrates the detailed spaceborne monitoring that is possible for examining spatial patterns of forest structure across the circumpolar

25 domain. The forest patch height prediction intervals are estimates of the measurement error at the forest patch scale that may help discern TTE form linked to changes in TTE forest structure.

BGD

doi:10.5194/bg-2015-575

Spaceborne potential for examining taiga-tundra ecotone form

P. M. Montesano et al.

We first discuss the utility of the patch-based analysis, review the patch-level estimates of uncertainty and then examine them in the context of a conceptual biogeographic model of TTE forest structure presented in recent literature. Such a model helps clarify and focus spaceborne approaches to examining characteristics of TTE forest structure and its vulnerability to change.

4.1 Patch-based TTE analysis

The patch-based approach of remotely measuring TTE forest structure addresses the imperative for site-scale detail of TTE vegetation, whereby individual trees can be resolved, while acknowledging the influence of clusters of trees (patches) and their density on TTE attributes and dynamics. This approach coarsens the data, reducing spatial detail. However, from a biogeographic perspective, this reduction in detail is not arbitrary as are image pixel reductions when images are coarsened by means of downsampling. Rather, image features and ancillary datasets inform the coarsening procedure, creating patch boundaries that are based on spectral and textural characteristics of images as well as other landscape information. Polygonal patches, particularly when vegetation patterns and heterogeneity are key landscape features, may be more informative than pixels particularly for studies at fine scales. Furthermore, patches provide a means to integrate remote sensing data across an area and extend sample measurements (Kellndorfer et al., 2010; Lefsky, 2010; Montesano et al., 2013; van Aardt et al., 2006; Wulder and Seemann, 2003; Wulder et al., 2007).

4.2 Forest patch height uncertainty

There are four central results regarding the uncertainty of forest patch height across the study area. The first two involve the sampling of canopy height within forest patches, while the last two focus on the its modeling. Theses local-scale results for the TTE are then put into context with existing global-scale estimates of forest height.

BGD

doi:10.5194/bg-2015-575

Spaceborne potential for examining taiga-tundra ecotone form

P. M. Montesano et al.

The way in which forest patch heights are sampled affects estimates. First, direct forest patch height estimates from a combination of coincident GLAS LiDAR ground surface and HRSI DSM-derived canopy elevations was made for ~ 9 % of forest patches in the study area. Second, the sampling density of these direct height estimates, driven by the sampling scheme of the spaceborne LiDAR, is < 0.5 samples ha^{-1} for 94 % of sampled patches. This sampling density is well below the critical density of 16 sample ha^{-1} recommended for sampling forest biomass at the 1 ha plot-scale (Huang et al., 2013). These results suggest that the cost of increasing forest patch sizes is a decrease in the density of direct height measurements. This is likely an artifact of the GLAS sampling scheme, whose sampling is regular in the along track direction (1 sample every ~ 170 m), but whose coverage of ground tracks was highly irregular across forested landscape.

The modeling of forest patch height provided some insight into the what drives the prediction of height and the associated uncertainty of predictions. First, the model that explained the most variation included all remote sensing data layers. However, this "all data" model showed little improvement on that built from HRSI predictors. Furthermore, in the former, the most important variables were from HRSI. These variables, NDVI and the standard deviation of the canopy surface roughness (SD_CSR), are indications of vegetation and its density within forest patches. This suggests that the medium-resolution data from ALOS and Landsat products are not strong predictors of vertical structure characteristics across the range of forest patch sizes identified in the study area, and that without HRSI inputs, the heterogeneity of TTE forest structure at the scale of its change across the ecological transition zone from forest to tundra is lost.

Second, the errors reported for the "all inputs" models predicting maximum and mean forest patch height show forest patch height errors, including error uncertainty at 2σ (95 % confidence interval) < 2 m. However, the prediction intervals for these vertical structure metrics show the uncertainty in the predictions on a patch by patch basis of ~ 40 %. These patch-level prediction intervals translate to a maximum patch height error of ±4 m for patches with maximum heights of 10 m. These errors indicate that

[BGD]

doi:10.5194/bg-2015-575

Spaceborne potential for examining taiga-tundra ecotone form

P. M. Montesano et al.

Discussion Paper | Discussion Paper | Discussion Paper | Discussion Paper

patches with maximum heights of 5 and 10 m would be statistically indistinguishable on the basis of height. This is a problem for identifying diffuse TTE forms, for which forest patch and tree height is a key attribute, because these forms generally features a gradual decrease of height and tree density across portions of the ecotone where present. Diffuse forms are the most likely type of general form to demonstrate treeline advance, where 80 % of diffuse ecotone sites examined in a meta-analysis show such treeline advance (Harsch et al., 2009).

These local-scale uncertainties improve upon recent global-scale spaceborne maps of vegetation height. These maps provide height uncertainties (RMSE) of ∼ 6 m which is expected given that coarse-scale (> 500 m) global maps of forest height aggregate many of these height measurement samples across broad spatial extents (Lefsky, 2010; Simard et al., 2011). This uncertainty can be the difference between the presence or absence of a forest patch in the TTE and is therefore not suited for evaluating the link between TTE forest structure and heterogeneous local-scale site factors. The height uncertainty of forest patches, ∼ 90 % of which have prediction intervals less than < 50 % of the predicted heights, improves the uncertainty and spatial resolution of TTE forest height measurements. However, this study's primary benefit is in the fidelity of the spatial extent of TTE forest patches. The scale of these patches are more appropriate than coarse, global-scale estimates of forest structure for reporting site-specific forest structure estimates that are critical for understanding forest characteristics at this biome boundary in flux.

4.3 Improving the depiction of forest patch height

A potentially large source of uncertainty of patch height estimates may be attributed to the use of direct height estimates for calibration of the indirect patch height prediction method. A patch's height was determined directly from coincident spaceborne sampling of canopy surface and ground elevations if samples were coincident with the patch. These patches with direct height samples were used to calibrate the Random Forest model relating a suite of satellite image data, averaged across the patch,

[BGD]

doi:10.5194/bg-2015-575

Spaceborne potential for examining taiga-tundra ecotone form

P. M. Montesano et al.

BGD

doi:10.5194/bg-2015-575

Spaceborne potential for examining taiga-tundra ecotone form

P. M. Montesano et al.

for indirectly predicting patch heights for those with no coincident direct spaceborne sampling of height. However, the sampling of patch height with coincident LiDAR footprints, which provided the ground surface elevation component of the sampled height estimate, involves sampling a very small portion of the overall patch. The assumption associated with delineating forest patches is that each patch itself is a homogenous unit with similar tree structure characteristics throughout. However, the extent to which this assumption holds was not examined. For patches with a high degree of tree structure heterogeneity, a single direct sample of height may not be sufficient to represent either maximum or mean patch heights. These data, when used to train a Random Forest model, will degrade the modeled relationship of mean patch level image characteristics to patch height, because the sample used to determine patch height might not be representative of actual patch height.

There are two ways to address this source of uncertainty. The first is to accumulate more direct samples of forest heights within a patch. This can be accomplished by first identifying ground surfaces within the forest patch and then by using the ground surface elevation measurements from the HRSI DSMs to supplement those from GLAS. This has to be done carefully so as not to introduce errors associated with HRSI DSM ground surface elevation within forested areas (Montesano et al., 2014b). Second, the homogeneity of forest patches can be improved by refining algorithms associated with delineating forest patches. This could include decreasing patch size, improving the canopy surface roughness algorithm, and including multi-temporal HRSI to help separate surface features whose reflectance characteristics differ throughout the growing season. These refinements may improve the modeling of forest patch height and ultimately the ability to discern diffuse TTE forms.

4.4 Spaceborne depiction of TTE form

The conceptual model of ecotone forms presented by Harsch and Bader (2011) describe form as a result of the relative dominance of different controlling mechanisms (Harsch and Bader, 2011). Only some of these mechanisms are primarily driven by cli-

mate. For the diffuse TTE form, the primary controlling mechanism of this conceptual pattern is the growth-limitation of trees, whereby tree-growth is driven by warming of summer or winter temperatures. Characterization of diffuse TTE forms by integrating horizontal and vertical structure by forest patch across the TTE with spaceborne data can provide insight into the vulnerability to climate warming of current TTE structure.

This study's spaceborne remote sensing analysis of height within forest patches provided a means to simultaneously account for the horizontal and vertical components of the spatial patterns of forest structure in the TTE that may help improve depictions of the diffuse TTE form. Recent literature on the patterns of trees in the TTE explain how tree density and height create varying forest patterns across the ecotone, that these patterns are important because they may provide clues as to the dynamics of TTE forest structure, and that they should be explored with detailed remote sensing (Bader et al., 2007; Harsch and Bader, 2011; Holtmeier and Broll, 2007).

A key element of this study involved integrating and scaling spatially detailed remote sensing observations to map forest patches. These mapped patches help explore the biogeography of TTE forest structure in the context of a conceptual model that highlights the importance of both tree density and height for examining patterns of trees in the TTE. From a remote sensing perspective, tree density is addressed with the delineation of forest patches that use the horizontal structure captured with HRSI. This horizontal structure manifests itself as image texture or the frequency of vegetation across a spatial extent, and may be quantified in terms of surface roughness, canopy cover or stem density. The patch-based approach for aggregating height information was a means to break apart the forested portions of each site by reducing the heterogeneity in horizontal structure. Essentially, the use of the roughness information derived from HRSI helped establish a basis for the analysis of height by using it as a proxy for vegetation density, and by expressing it as a contiguous patch that served as the fundamental unit by which height was aggregated. This data integration should provide more information for discerning diffuse TTE forms than individual assessments of either tree height or tree density. Finally, the integration of spaceborne data across

[BGD](#)

doi:10.5194/bg-2015-575

Spaceborne potential for examining taiga-tundra ecotone form

P. M. Montesano et al.

a range of scales is critical. This suite of data that is available for the entire TTE enables a standardized approach to TTE structure mapping that is appropriate for the broad spatial domain of the TTE while adhering to requirements of site-specific forest structure detail.

5   The site-scale, patch-based treatment of the landscape is driven by two central needs. The first is the need for site-level understanding of TTE vegetation structure characteristics. The second is the need to understand the hierarchy of spatial patterns of trees across the landscape, because of the link between vegetation patterns and ecological processes. This analytical approach should be developed to more deeply

10 explore the TTE vegetation patterns that variations in height and density reveal, such as patch size, shape, landscape position, connectivity and spatial autocorrelation of varying types of forest patches across the TTE as well as the association of such patterns with permafrost dynamics.

4.5 Implications for understanding TTE structure vulnerability

15 Understanding the vulnerability of TTE structure is a key objective of research into expected changes in the high northern latitudes (Callaghan et al., 2002a). Vulnerability may be defined as the susceptibility of vegetation structure within the TTE to change, thus shifting the position and character of the TTE (Gonzalez et al., 2010). Multiple lines of evidence indicate that vegetation changes are occurring in the TTE, and that

20 these changes are asynchronous across the circumpolar domain. The most rapid TTE vegetation responses to climate change will occur where climate is the main factor controlling TTE vegetation (Epstein et al., 2004). This suggests that TTE structure is most vulnerable at sites both controlled by, and undergoing changes in, climate. Currently, the reported patch-level forest height uncertainty precludes a clear understanding of

25 the most vulnerable portions of the TTE. However, this spaceborne approach framed by the conceptual model of TTE form provides a clear directive for near-term work of examining the biogeography of forest structure in the TTE, and understanding and

[BGD]

doi:10.5194/bg-2015-575

Spaceborne potential for examining taiga-tundra ecotone form

P. M. Montesano et al.

Discussion Paper | Discussion Paper | Discussion Paper | Discussion Paper | Discussion Paper |

forecasting vegetation responses in the TTE based on the potential for changes (i.e. vulnerability) that these general patterns of forest structure suggest.

Mapped TTE patterns of horizontal and vertical structure, i.e. TTE form, would be useful for examining ecosystem dynamics in the HNL. These maps could be integrated with topographic, hydrologic, permafrost and other climate data to suggest a gradient of TTE structure vulnerability. They would (i) provide information on the patterns of environmental variables that are the dominant drivers of tree growth, (ii) provide insight into the influence of TTE structural changes on HNL biodiversity (Hofgaard et al., 2012), and (iii) inform plant community and forest gap models that combine temperature, soil and disturbance data to examine the drivers of vegetation structure and forecast its potential for change in the TTE (Epstein et al., 2000; Xiaodong and Shugart, 2005). For example, understanding form in areas where vegetation structural changes have been noted may help explain the variability of structure change.

It is unlikely that the dominant mechanisms controlling TTE forest structure will be derived directly from remote sensing. However, these mechanisms may be inferred from remotely sensed TTE form. Resolving diffuse TTE forms through better forest patch height estimates provide evidence as to the general mechanisms that give rise to these diffuse forms (e.g. temperature-limited growth), and could also provide spatially explicit information to individual-based models to help account for the variability in TTE forest structure responses across the circumpolar domain. This will aid long-term forecasting by suggesting the most likely sites, at fine scales, for changes to vegetation-disturbance feedbacks and the extent to which biogeophysical interactions may shift (e.g. vegetation effects on surface albedo). The vulnerability of TTE structure to temperature-induced change is one of many factors that may alter ecological processes in the high northern latitudes.

[BGD](#)

doi:10.5194/bg-2015-575

Spaceborne potential for examining taiga-tundra ecotone form

P. M. Montesano et al.

5   Conclusions

The vertical component of TTE form, maximum and mean forest patch height, as derived from a suite of spaceborne sensors, has an uncertainty of $\sim 40\,\%$. With this uncertainty, forest patches with maximum heights of 5 and 10 m are statistically indistinguishable on the basis of height. Height is a key attribute of the diffuse TTE forms, which generally feature a gradual decrease of height and tree density across the ecotone and are the most likely form to demonstrate treeline advance. Differences in patch height are a central feature of the diffuse TTE form where significant structural changes have been observed, and these differences suggests that improving the remote sensing of patch height is a key TTE forest structure variable for examining TTE structure vulnerability to temperature-induced change. The conceptual model of TTE form should continue to guide the application of multi-sensor spaceborne data in the HNL toward classifying the TTE according to form. These forms can be more informative than tree density and height alone, because of the information provided by the structural patterns of groups of forest patches. This work clarifies how improved height estimates at the scale of forest patches can help capture a key characteristic of TTE vulnerability – the portions of the TTE for which temperature is likely the primary control of forest structure. A focus on forest patch height from spaceborne data will provide domain-wide potential for examining TTE structure characteristics.

References

Bader, M. Y., Rietkerk, M., and Bregt, A. K.: Vegetation structure and temperature regimes of tropical alpine treelines, Arct. Antarct. Alp. Res., 39, 353–364, doi:10.1657/1523-0430(06-055)[BADER]2.0.CO;2, 2007.

Bekker, M. F.: Positive feedback between tree establishment and patterns of subalpine forest advancement, Glacier National Park, Montana, USA, Arct. Antarct. Alp. Res., 37, 97–107, 2005.

Discussion Paper | Discussion Paper | Discussion Paper | Discussion Paper |

[BGD](#)

doi:10.5194/bg-2015-575

Spaceborne potential for examining taiga-tundra ecotone form

P. M. Montesano et al.

Interactive Discussion

Benz, U. C., Hofmann, P., Willhauck, G., Lingenfelder, I., and Heynen, M.: Multi-resolution, object-oriented fuzzy analysis of remote sensing data for GIS-ready information, ISPRS J. Photogramm., 58, 239–258, doi:10.1016/j.isprsjprs.2003.10.002, 2004.

Bonan, G. B.: Forests and climate change: forcings, feedbacks, and the climate benefits of forests, Science, 320, 1444–1449, doi:10.1126/science.1155121, 2008.

Bondarev, A.: Age distribution patterns in open boreal Dahurican larch forests of Central Siberia, Forest Ecol. Manag., 93, 205–214, 1997.

Bonfils, C. J. W., Phillips, T. J., Lawrence, D. M., Cameron-Smith, P., Riley, W. J., and Subin, Z. M.: On the influence of shrub height and expansion on northern high latitude climate, Environ. Res. Lett., 7, 015503, doi:10.1088/1748-9326/7/1/015503, 2012.

Breiman, L.: Random forests, Mach. Learn., 45, 5–32, 2001.

Callaghan, T. V., Crawford, R. M., Eronen, M., Hofgaard, A., Payette, S., Rees, W. G., Skre, O., Sveinbjörnsson, B., Vlassova, T. K., and Werkman, B. R.: The dynamics of the tundra-taiga boundary: an overview and suggested coordinated and integrated approach to research, Ambio, Special Report 12, 3–5, 2002a.

Callaghan, T. V., Werkman, B. R., and Crawford, R. M.: The tundra-taiga interface and its dynamics: concepts and applications, Ambio, Special Report 12, 6–14, 2002b.

Callaghan, T. V., Bergholm, F., Christensen, T. R., Jonasson, C., Kokfelt, U., and Johansson, M.: A new climate era in the sub-Arctic: accelerating climate changes and multiple impacts, Geophys. Res. Lett., 37, L14705, doi:10.1029/2009GL042064, 2010.

D'Odorico, P., He, Y., Collins, S., De Wekker, S. F. J., Engel, V., and Fuentes, J. D.: Vegetation-microclimate feedbacks in woodland-grassland ecotones, Global Ecol. Biogeogr., 22, 364–379, doi:10.1111/geb.12000, 2012.

Dalen, L. and Hofgaard, A.: Differential regional treeline dynamics in the Scandes Mountains, Arct. Antarct. Alp. Res., 37, 284–296, 2005.

Danby, R. K. and Hik, D. S.: Variability, contingency and rapid change in recent subarctic alpine tree line dynamics, J. Ecol., 95, 352–363, doi:10.1111/j.1365-2745.2006.01200.x, 2007.

Davis, R. E., Hardy, J. P., Ni, W., Woodcock, C., McKenzie, J. C., Jordan, R., and Li, X.: Variation of snow cover ablation in the boreal forest: a sensitivity study on the effects of conifer canopy, J. Geophys. Res.-Atmos., 102, 29389–29395, 1997.

Dufour-Tremblay, G., Lévesque, E., and Boudreau, S.: Dynamics at the treeline: differential responses of Picea mariana and Larix laricinato climate change in eastern subarctic Québec, Environ. Res. Lett., 7, 044038, doi:10.1088/1748-9326/7/4/044038, 2012.

BGD

doi:10.5194/bg-2015-575

Spaceborne potential for examining taiga-tundra ecotone form

P. M. Montesano et al.

Epstein, H. E., Walker, M. D., Chapin III, F. S., and Starfield, A. M.: A transient, nutrient-based model of arctic plant community response to climatic warming, Ecol. Appl., 10, 824–841, 2000.

Epstein, H. E., Beringer, J., Gould, W. A., Lloyd, A. H., Thompson, C. D., Chapin, F. S., Michaelson, G. J., Ping, C. L., Rupp, T. S., and Walker, D. A.: The nature of spatial transitions in the Arctic, J. Biogeogr., 31, 1917–1933, 2004.

Frost, G. V., Epstein, H. E., and Walker, D. A.: Regional and landscape-scale variability of landsat-observed vegetation dynamics in northwest Siberian tundra, Environ. Res. Lett., 9, 025004, doi:10.1088/1748-9326/9/2/025004, 2014.

Gonzalez, P., Neilson, R. P., Lenihan, J. M., and Drapek, R. J.: Global patterns in the vulnerability of ecosystems to vegetation shifts due to climate change, Global Ecol. Biogeogr., 19, 755–768, doi:10.1111/j.1466-8238.2010.00558.x, 2010.

Hansen, M. C., Potapov, P. V., Moore, R., Hancher, M., Turubanova, S. A., Tyukavina, A., Thau, D., Stehman, S. V., Goetz, S. J., Loveland, T. R., Kommareddy, A., Egorov, A., Chini, L., Justice, C. O., and Townshend, J. R. G.: High-resolution global maps of 21st-century forest cover change, Science, 342, 850–853, doi:10.1126/science.1244693, 2013.

Hansen-Bristow, K. J. and Ives, J. D.: Composition, form, and distribution of the forest-alpine tundra ecotone, Indian Peaks, Colorado, USA (Zusammensetzung, Form und Verbreitung des Übergangssaumes zwischen der Waldstufe und der alpinen Tundrastufe im Indian Peaks Gebiet, Front Range, Colorado, USA), Erdkunde, 286–295, 1985.

Hardy, J. P., Davis, R. E., Jordan, R., Ni, W., and Woodcock, C. E.: Snow ablation modelling in a mature aspen stand of the boreal forest, Hydrol. Process., 12, 1763–1778, 1998.

Harper, K. A., Danby, R. K., De Fields, D. L., Lewis, K. P., Trant, A. J., Starzomski, B. M., Savidge, R., and Hermanutz, L.: Tree spatial pattern within the forest–tundra ecotone: a comparison of sites across Canada, Can. J. Forest Res., 41, 479–489, doi:10.1139/X10-221, 2011.

Harsch, M. A. and Bader, M. Y.: Treeline form – a potential key to understanding treeline dynamics, Global Ecol. Biogeogr., 20, 582–596, doi:10.1111/j.1466-8238.2010.00622.x, 2011.

Harsch, M., Hulme, P., McGlone, M., and Duncan, R.: Are treelines advancing? A global meta-analysis of treeline response to climate warming, Ecol. Lett., 12, 1040–1049, 2009.

Haugo, R. D., Halpern, C. B., and Bakker, J. D.: Landscape context and long-term tree influences shape the dynamics of forest-meadow ecotones in mountain ecosystems, Ecosphere, 2, 91, doi:10.1890/ES11-00110.1, 2011.

BGD

doi:10.5194/bg-2015-575

Spaceborne potential for examining taiga-tundra ecotone form

P. M. Montesano et al.

Hofgaard, A., Dalen, L., and Hytteborn, H.: Tree recruitment above the treeline and potential for climate-driven treeline change, J. Veg. Sci., 20, 1133–1144, 2009.

Hofgaard, A., Harper, K. A., and Golubeva, E.: The role of the circumarctic forest–tundra ecotone for Arctic biodiversity, Biodiversity, 13, 174–181, doi:10.1080/14888386.2012.700560, 2012.

Holtmeier, F.-K. and Broll, G.: Sensitivity and response of Northern Hemisphere altitudinal and polar treelines to environmental change at landscape and local scales, Global Ecol. Biogeogr., 14, 395–410, 2005.

Holtmeier, F.-K. and Broll, G.: Treeline advance – driving processes and adverse factors, Landscape Online, 1, 1–32, doi:10.3097/LO.200701, 2007.

Holtmeier, K.-F. and Broll, G.: Altitudinal and polar treelines in the Northern Hemisphere causes and response to climate change (Obere und polare Baumgrenze auf der nördlichen Hemisphäre Ursachen und Antwort auf den Klimawandel), Polarforschung, 79, 139–153, 2010.

Huang, W., Sun, G., Dubayah, R., Cook, B., Montesano, P., Ni, W., and Zhang, Z.: Mapping biomass change after forest disturbance: Applying LiDAR footprint-derived models at key map scales, Remote Sens. Environ., 134, 319–332, doi:10.1016/j.rse.2013.03.017, 2013.

Johansen, K., Sohlbach, M., Sullivan, B., Stringer, S., Peasley, D., and Phinn, S.: Mapping banana plants from high spatial resolution orthophotos to facilitate plant health assessment, Remote Sensing, 6, 8261–8286, doi:10.3390/rs6098261, 2014.

Kellndorfer, J. M., Walker, W. S., LaPoint, E., Kirsch, K., Bishop, J., and Fiske, G.: Statistical fusion of lidar, InSAR, and optical remote sensing data for forest stand height characterization: a regional-scale method based on LVIS, SRTM, Landsat ETM plus, and ancillary data sets, J. Geophys. Res.-Biogeo., 115, G00E08, doi:10.1029/2009JG000997, 2010.

Kent, M., Gill, W. J., Weaver, R. E., and Armitage, R. P.: Landscape and plant community boundaries in biogeography, Prog. Phys. Geog., 21, 315–353, 1997.

Kharuk, V., Ranson, K., and Dvinskaya, M. L.: Evidence of evergreen conifer invasion into larch dominated forests during recent decades in Central Siberia, Eurasian Journal of Forest Research, 10, 163–171, 2007.

Le Toan, T., Quegan, S., Davidson, M. W. J., Balzter, H., Paillou, P., Papathanassiou, K., Plummer, S., Rocca, F., Saatchi, S., Shugart, H., and Ulander, L.: The BIOMASS mission: Mapping global forest biomass to better understand the terrestrial carbon cycle, Remote Sens. Environ., 115, 2850–2860, doi:10.1016/j.rse.2011.03.020, 2011.

BGD

doi:10.5194/bg-2015-575

Spaceborne potential for examining taiga-tundra ecotone form

P. M. Montesano et al.

Lefsky, M. A.: A global forest canopy height map from the moderate resolution imaging spectroradiometer and the geoscience laser altimeter system, Geophys. Res. Lett., 37, L15401, doi:10.1029/2010GL043622, 2010.

Lloyd, A. H., Rupp, T. S., Fastie, C. L., and Starfield, A. M.: Patterns and dynamics of treeline advance on the Seward Peninsula, Alaska, J. Geophys. Res., 108, 8161, doi:10.1029/2001JD000852, 2002.

Lloyd, A. H., Yoshikawa, K., Fastie, C. L., Hinzman, L., and Fraver, M.: Effects of permafrost degradation on woody vegetation at arctic treeline on the Seward Peninsula, Alaska, Permafrost Periglac., 14, 93–101, doi:10.1002/ppp.446, 2003.

Loranty, M. M., Berner, L. T., Goetz, S. J., Jin, Y., and Randerson, J. T.: Vegetation controls on northern high latitude snow-albedo feedback: observations and CMIP5 model predictions, Glob. Change Biol., 20, 594–606, doi:10.1111/gcb.12391, 2013.

Malanson, G. P., Zeng, Y., and Walsh, S. J.: Complexity at advancing ecotones and frontiers, Environ. Plann. A, 38, 619–632, doi:10.1068/a37340, 2006.

Mathisen, I. E., Mikheeva, A., Tutubalina, O. V., Aune, S., and Hofgaard, A.: Fifty years of tree line change in the Khibiny Mountains, Russia: advantages of combined remote sensing and dendroecological approaches, edited by: Rocchini, D., Appl. Veg. Sci., 17, 6–16, doi:10.1111/avsc.12038, 2013.

Mette, T., Papathanassiou, K., and Hajnsek, I.: Biomass estimation from polarimetric SAR interferometry over heterogeneous forest terrain, Geoscience and Remote Sensing Symposium, 2004 IGARSS'04 Proceedings, 20–24 September 2004, IEEE International, 1, 511–514, 2004.

Montesano, P. M., Cook, B. D., Sun, G., Simard, M., Nelson, R. F., Ranson, K. J., Zhang, Z., and Luthcke, S.: Achieving accuracy requirements for forest biomass mapping: a spaceborne data fusion method for estimating forest biomass and LiDAR sampling error, Remote Sens. Environ., 130, 153–170, doi:10.1016/j.rse.2012.11.016, 2013.

Montesano, P. M., Nelson, R. F., Dubayah, R. O., Sun, G., Cook, B. D., Ranson, K., Næsset, E., and Kharuk, V.: The uncertainty of biomass estimates from LiDAR and SAR across a boreal forest structure gradient, Remote Sens. Environ., 154, 398–407, doi:10.1016/j.rse.2014.01.027, 2014a.

Montesano, P. M., Rosette, J., Sun, G., North, P., Nelson, R. F., Dubayah, R. O., Ranson, K. J., and Kharuk, V.: The uncertainty of biomass estimates from modeled

ICESat-2 returns across a boreal forest gradient, Remote Sens. Environ., 158, 95–109, doi:10.1016/j.rse.2014.10.029, 2015.

Montesano, P., Sun, G., Dubayah, R., and Ranson, K.: The uncertainty of plot-scale forest height estimates from complementary spaceborne observations in the Taiga-Tundra Ecotone, R emote Sensing, 6, 10070–10088, doi:10.3390/rs61010070, 2014b.

Naurzbaev, M. M. and Vaganov, E. A.: Variation of early summer and annual temperature in east Taymir and Putoran (Siberia) over the last two millennia inferred from tree rings, J. Geophys. Res.-Atmos., 105, 7317–7326, 2000.

Naurzbaev, M. M., Hughes, M. K., and Vaganov, E. A.: Tree-ring growth curves as sources of climatic information, Quaternary Res., 62, 126–133, doi:10.1016/j.yqres.2004.06.005, 2004.

Neigh, C. S., Masek, J. G., and Nickeson, J. E.: High-resolution satellite data open for government research, Eos, Transactions American Geophysical Union, 94, 121–123, 2013.

Ni, W. and Woodcock, C. E.: Effect of canopy structure and the presence of snow on the albedo of boreal conifer forests, J. Geophys. Res.-Atmos., 105, 11879–11888, 2000.

Ni, W., Li, X., Woodcock, C. E., Roujean, J. L., and Davis, R. E.: Transmission of solar radiation in boreal conifer forests: measurements and models, J. Geophys. Res.-Atmos., 102, 29555–29566, 1997.

Ni-Meister, W. and Gao, H.: Assessing the impacts of vegetation heterogeneity on energy fluxes and snowmelt in boreal forests, J. Plant Ecol.-UK, 4, 37–47, doi:10.1093/jpe/rtr004, 2011.

Osawa, A. and Kajimoto, T.: Development of Stand Structure in Larch Forests, in: Ecological Studies, Vol. 209, 123–148, Ecological Studies, Dordrecht, 2009.

Roy-Léveillée, P., Burn, C. R., and McDonald, I. D.: Vegetation-permafrost relations within the forest-tundra ecotone near Old Crow, Northern Yukon, Canada, Permafrost Periglac., 25, 127–135, 2014.

Shamsoddini, A. and Trinder, J. C.: Edge-detection-based filter for SAR speckle noise reduction, Int. J. Remote Sens., 33, 2296–2320, doi:10.1080/01431161.2011.614286, 2012.

Shimada, M., Itoh, T., Motooka, T., Watanabe, M., Shiraishi, T., Thapa, R., and Lucas, R.: New global forest/non-forest maps from ALOS PALSAR data (2007–2010), Remote Sens. Environ., 155, 13–31, doi:10.1016/j.rse.2014.04.014, 2014.

Simard, M., Pinto, N., and Fisher, J.: Mapping forest canopy height globally with spaceborne lidar, J. Geophys. Res., 116, G04021, doi:10.1029/2011JG001708, 2011.

BGD

doi:10.5194/bg-2015-575

Spaceborne potential for examining taiga-tundra ecotone form

P. M. Montesano et al.

van Aardt, J., Wynne, R., and Oderwald, R.: Forest volume and biomass estimation using small-footprint lidar-distributional parameters on a per-segment basis, Forest Sci., 52, 636–649, 2006.

Virtanen, R., Luoto, M., Rämä, T., Mikkola, K., Hjort, J., Grytnes, J.-A., and Birks, H. J. B.: Recent vegetation changes at the high-latitude tree line ecotone are controlled by geo-morphological disturbance, productivity and diversity, Global Ecol. Biogeogr., 19, 810–821, doi:10.1111/j.1466-8238.2010.00570.x, 2010.

Wulder, M. A. and Seemann, D.: Forest inventory height update through the integration of lidar data with segmented Landsat imagery, Can. J. Remote Sens., 29, 536–543, 2003.

Wulder, M., Han, T., White, J., Sweda, T., and Tsuzuki, H.: Integrating profiling LIDAR with Land-sat data for regional boreal forest canopy attribute estimation and change characterization, Remote Sens. Environ., 110, 123–137, 2007.

Xiaodong, Y. and Shugart, H. H.: FAREAST: a forest gap model to simulate dynamics and patterns of eastern Eurasian forests, J. Biogeogr., 32, 1641–1658, doi:10.1111/j.1365-2699.2005.01293.x, 2005.

Zhang, Y.: Sublimation from snow surface in southern mountain taiga of eastern Siberia, J. Geophys. Res., 109, D21103, doi:10.1029/2003JD003779, 2004.

Discussion Paper | Discussion Paper | Discussion Paper | Discussion Paper |

BGD

doi:10.5194/bg-2015-575

Spaceborne potential for examining taiga-tundra ecotone form

P. M. Montesano et al.

BGD

doi:10.5194/bg-2015-575

Spaceborne potential for examining taiga-tundra ecotone form

P. M. Montesano et al.

Discussion Paper | Discussion Paper | Discussion Paper | Discussion Paper | Discussion Paper

Table 1. Summary of spaceborne image datasets used to delineate or attribute forest patches.

Dataset	Date	Attribute	Scale
Landsat-7 cloud-free composite, percent tree cover	c. 2013	Top-of-atmosphere reflectance (SWIR, NIR, red, green); tree cover	30 m pixel
HRSI: WorldView 1 and 2	c. 2012	DSM, NDVI, roughness, CRM	~ 0.5–2 m pixel
ALOS PALSAR composite	2007–2010	backscatter power (HH, HV)	25 m pixel
ICESat-GLAS LiDAR	2003–2006	ground surface elevation, waveform length	~ 60 m diameter footprint
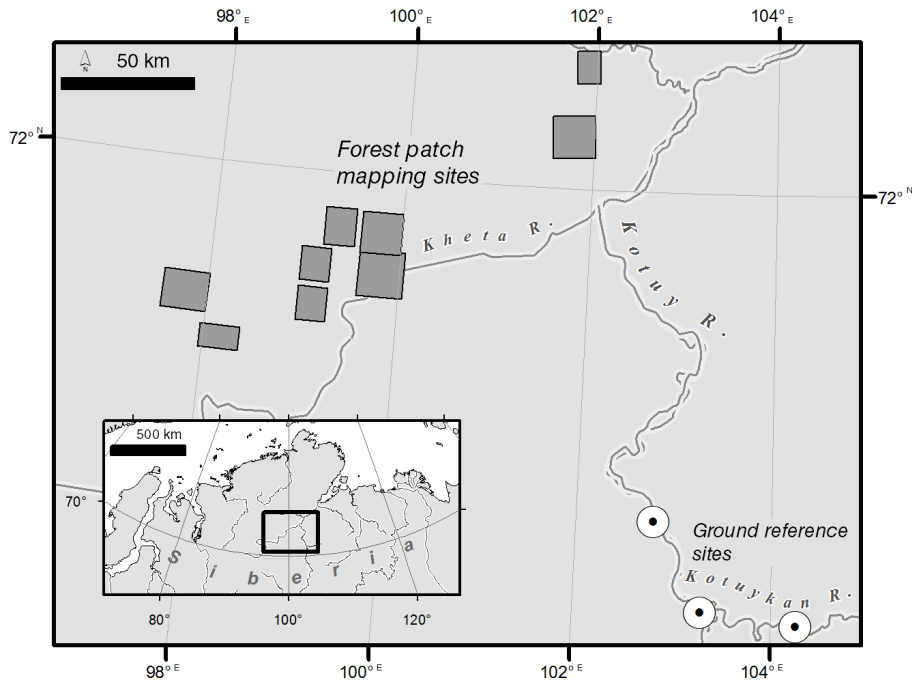
Figure 1. Study area in northern Siberia showing the 9 forest patch mapping sites (boxes) and the ground reference sites along the Kotuykan River (circles) at which individual tree height measurements in circular plots coincident with ICESat-GLAS LiDAR footprints were collected.

Discussion Paper | Discussion Paper | Discussion Paper | Discussion Paper |

BGD

doi:10.5194/bg-2015-575

Spaceborne potential for examining taiga-tundra ecotone form

P. M. Montesano et al.

BGD

doi:10.5194/bg-2015-575

Spaceborne potential for examining taiga-tundra ecotone form

P. M. Montesano et al.
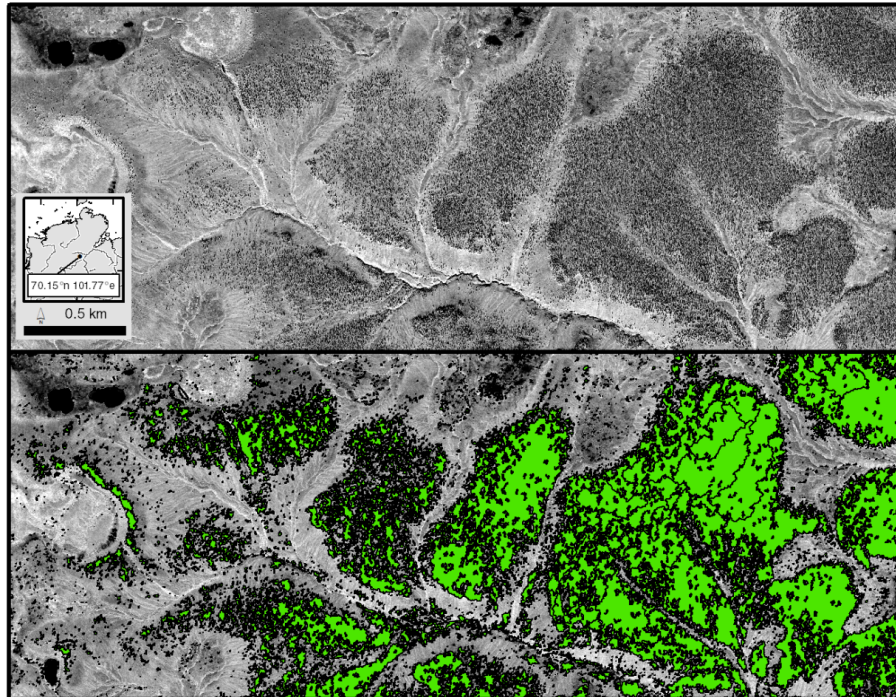
Figure 2. A representative example of diffuse forest patches across an upland site delineated from HRSI. The top image shows a subset of a Worldview-1 panchromatic image from 21 August 2012 in one of the forest patch mapping sites. The bottom image shows the same subset with forest patches overlaid (green with black outline).

BGD

doi:10.5194/bg-2015-575

Spaceborne potential for examining taiga-tundra ecotone form

P. M. Montesano et al.
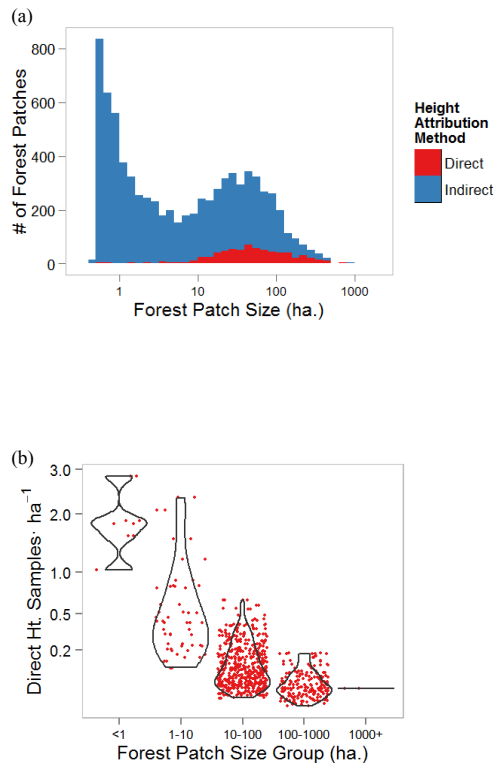
Figure 3. (a) The distributions of forest patch size in hectares according to height attribution method. **(b)** The distribution of direct height sample density (shown as violin plots) for each forest patch size group, overlain with dots representing individual patches (red).

BGD

doi:10.5194/bg-2015-575

Spaceborne potential for examining taiga-tundra ecotone form

P. M. Montesano et al.
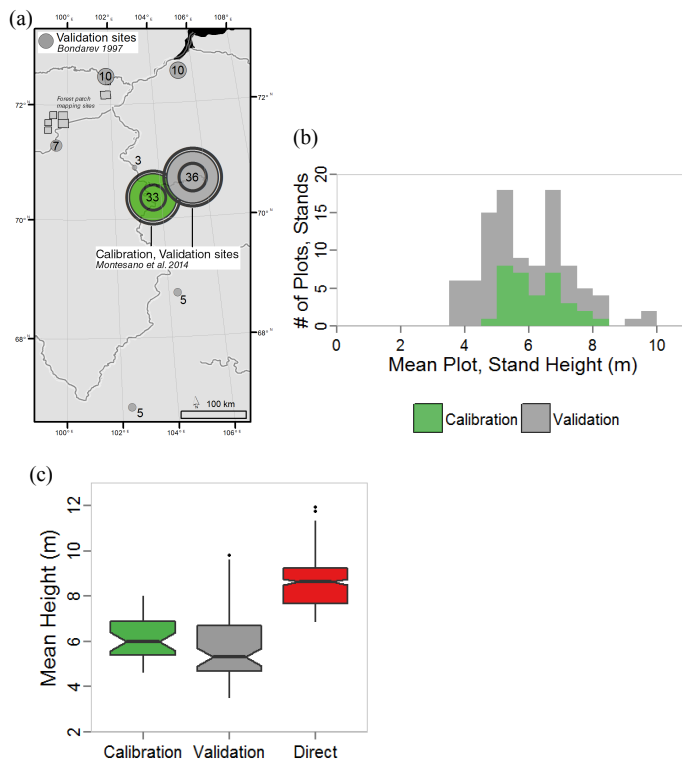
Figure 4. **(a)** Histogram of mean plot and stand heights from calibration and validation data. **(b)** Map of locations of calibration (green) and validation (grey) sites in northern Siberia with the number of stands or plots associated with each site. The circles representing general site locations are sized according to the number of stands. **(c)** Notched boxplots showing the 25th, 50th, and 75th percentiles as horizontal lines and 1.5 times the inter-quartile range as vertical lines. Notches roughly indicate the 95 % confidence interval for the median.

BGD

doi:10.5194/bg-2015-575

Spaceborne potential for examining taiga-tundra ecotone form

P. M. Montesano et al.
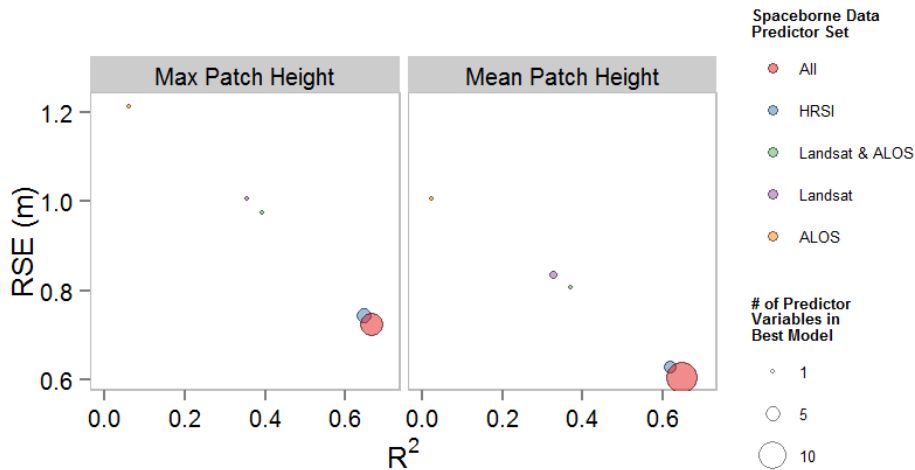
Figure 5. Results from Random Forest indirect forest patch height estimation for 5 spaceborne data predictor sets.

BGD

doi:10.5194/bg-2015-575

Spaceborne potential
for examining
taiga-tundra ecotone
form

P. M. Montesano et al.

(a)

(b)
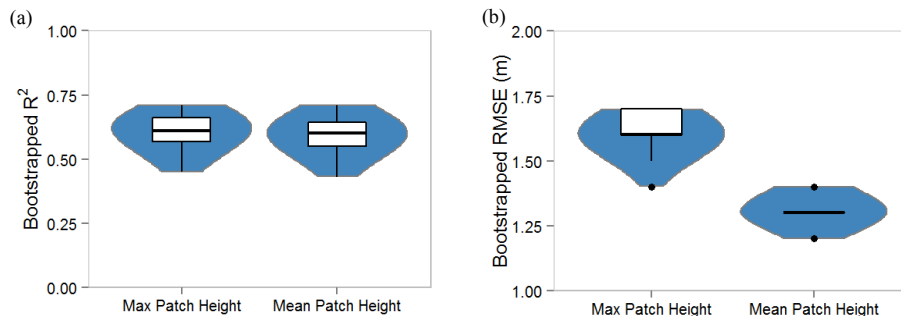
Figure 6. The bootstrap-derived distributions (shown as violin plots, blue) of the Random Forest model's **(a)** R^2 and **(b)** RMSE for the indirect forest patch height prediction method whereby all spaceborne variables were used to predict maximum and mean forest patch height. Boxplots (white) show the 25th and 75th percentiles (lower and upper lines), median (dark line), and 1.5× the inter-quartile range (whiskers). Data beyond the whiskers are shown as points.

Discussion Paper | Discussion Paper | Discussion Paper | Discussion Paper |

BGD

doi:10.5194/bg-2015-575

Spaceborne potential for examining taiga-tundra ecotone form

P. M. Montesano et al.
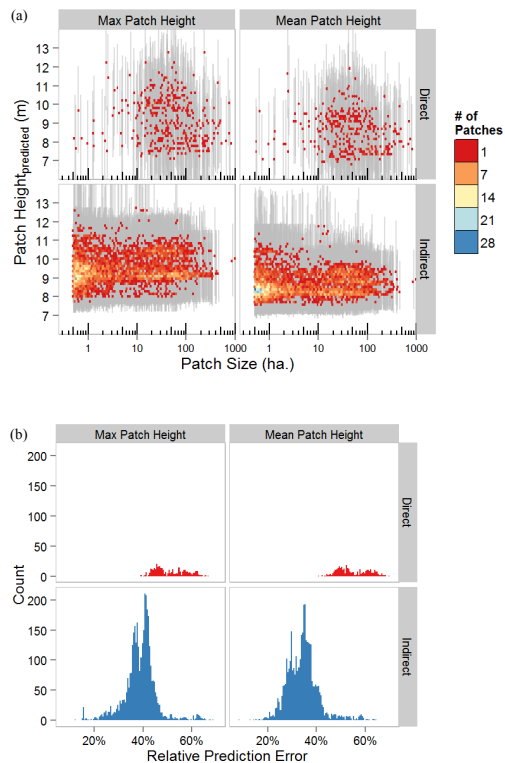
Figure 7. (a) Patch height and 95 % prediction intervals (grey lines) for patches from direct prediction and indirect prediction shown across the continuum of patch sizes. **(b)** Distributions of relative prediction error (95 % prediction interval) for patch height predictions.